



ELSEVIER

Contents lists available at ScienceDirect

## Data in brief

journal homepage: [www.elsevier.com/locate/dib](http://www.elsevier.com/locate/dib)



### Data Article

# Datasets acquired with correlative microscopy method for delineation of prior austenite grain boundaries and characterization of prior austenite grain size in a low-alloy high-performance steel



V. Sinha <sup>a, b, \*</sup>, M. Gonzales <sup>a</sup>, E.J. Payton <sup>a</sup>

<sup>a</sup> Air Force Research Laboratory, Materials and Manufacturing Directorate, AFRL/RXCM, Wright-Patterson Air Force Base, OH 45433, USA

<sup>b</sup> UES, Inc., 4401 Dayton-Xenia Road, Dayton, OH 45432, USA

#### ARTICLE INFO

##### Article history:

Received 25 July 2019

Received in revised form 12 August 2019

Accepted 26 August 2019

Available online 3 September 2019

##### Keywords:

Martensitic steel

Chemical etching

Scanning electron microscopy

Electron backscatter diffraction (EBSD)

Prior austenite grain boundary (PAGB)

#### ABSTRACT

Prior studies on martensitic steel microstructures have either delineated the prior austenite grain boundaries via chemical etching or reconstructed the prior austenite grains from crystallographic orientations measured with electron backscattered diffraction (EBSD). To appropriately validate the reconstruction algorithms, the EBSD data need to be collected on martensitic microstructures, where the prior austenite grain boundaries are delineated with techniques such as chemical etching that can serve as ground truth for comparison with the reconstructed prior austenite grains. In this article, the method of correlative microscopy is employed to collect scanning electron microscope (SEM) image and automated EBSD scan data from the same region of an appropriately etched steel specimen. The SEM images and automated EBSD scan data are presented for five different fields of view in the specimen. These datasets are analyzed and discussed in the

DOI of original article: <https://doi.org/10.1016/j.matchar.2019.109835>.

\* Corresponding author. Air Force Research Laboratory, Materials and Manufacturing Directorate, AFRL/RXCM, Wright-Patterson Air Force Base, OH, 45433, USA.

E-mail address: [vikas.sinha.1.ctr@us.af.mil](mailto:vikas.sinha.1.ctr@us.af.mil) (V. Sinha).

<https://doi.org/10.1016/j.dib.2019.104471>

2352-3409/© 2019 Published by Elsevier Inc. This is an open access article under the CC BY-NC-ND license (<http://creativecommons.org/licenses/by-nc-nd/4.0/>).

accompanying article titled “Correlative microscopy for quantification of prior austenite grain size in AF9628 steel” [1].

© 2019 Published by Elsevier Inc. This is an open access article under the CC BY-NC-ND license (<http://creativecommons.org/licenses/by-nc-nd/4.0/>).

#### Specifications Table

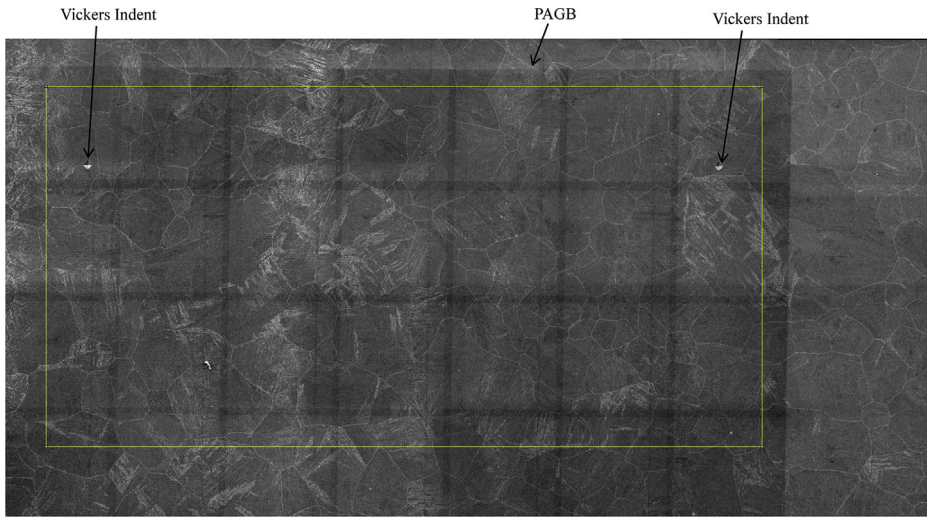
Subject area	Materials Science and Engineering
More specific subject area	Metals and Alloys
Type of data	Table, SEM image, EBSD orientation map, EBSD data file, text file, figure
How data was acquired	SEM imaging, EBSD
Data format	Raw, processed, analyzed
Experimental factors	Sample was prepared via metallographic polishing and swab etched for 3 minutes with a solution of 100 ml saturated aqueous picric acid and 0.5 g sodium dodecyl benzene sulfonate (a wetting agent).
Experimental features	Chemical etching revealed the prior austenite grain boundaries, when the etched sample was examined under an SEM with a secondary electron detector. The polished and etched specimen was also amenable for characterization with EBSD. The SEM image and the EBSD orientation map were collected for the same region on the specimen.
Data source location	The datasets were collected at the Air Force Research Laboratory, Materials and Manufacturing Directorate, AFRL/RXCM, Wright-Patterson Air Force Base, OH, USA.
Data accessibility	The data are included in this article. The high resolution SEM images and the EBSD data (*.ang) files can be accessed at <a href="https://doi.org/10.18126/iv89-3293">https://doi.org/10.18126/iv89-3293</a>
Related research article	V. Sinha, M. Gonzales, R.A. Abrahams, B.S. Song, and E.J. Payton, “Correlative microscopy for quantification of prior austenite grain size in AF9628 steel”, <i>Materials Characterization</i> , 2019 (In Press), DOI: <a href="https://doi.org/10.1016/j.matchar.2019.109835">https://doi.org/10.1016/j.matchar.2019.109835</a>

#### Value of the Data

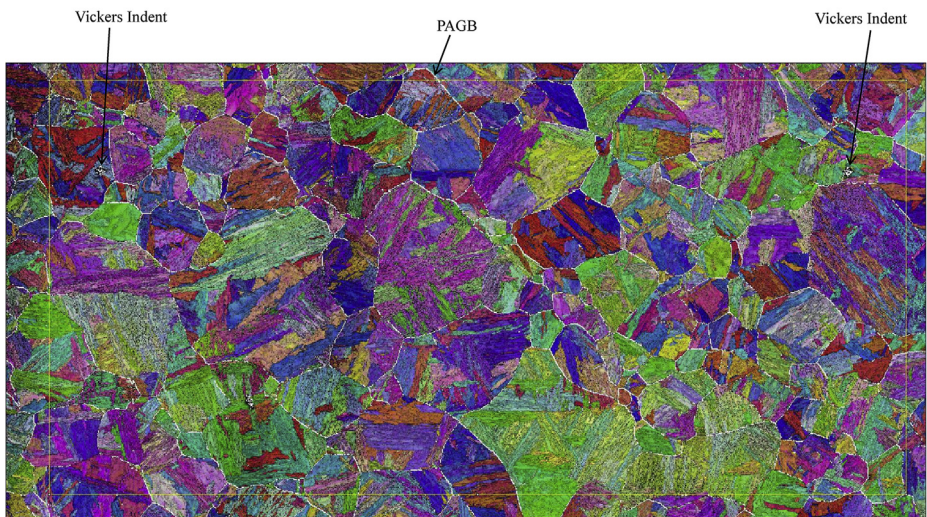
- The EBSD data can be utilized to reconstruct the prior austenite grains with the reconstruction algorithms such as those reported in Refs. [2–4].
- The SEM images can serve as a ground truth to benchmark the results of reconstruction algorithms.
- The reconstructed prior austenite grains and grain boundaries can be compared and contrasted with the SEM images of the same areas on the specimen, where the prior austenite grain boundaries are delineated by an independent method of chemical etching.
- The reported EBSD data and SEM images from correlative microscopy experiments are expected to be quite valuable in validating the reconstruction algorithms.
- The reported datasets are also likely to be valuable in further development and refinement of reconstruction algorithms.

## 1. Data

The SEM images and the corresponding EBSD orientation maps are provided for five different fields of view on an etched steel sample. The prior austenite grain boundaries (PAGBs) are delineated via chemical etching in the SEM images and via misorientation thresholding in the EBSD maps. The field of view 1 is outlined by a yellow rectangle in the large area SEM image (Fig. 1(a)) and the corresponding EBSD orientation map (Fig. 1(b)). The SEM image and EBSD map for the cropped region (i.e., field of view 1) are presented in Ref. [1] as Figs. 4 and 6, respectively. The horizontal and vertical gridlines overlaid on the cropped SEM image and EBSD map are shown in Fig. 7 of Ref. [1]. The results of stereological analyses on SEM image and EBSD map for field of view ‘1’ are presented in Table 2 of Ref. [1].



(a) SEM image (Size of yellow rectangle =  $923.1 \mu\text{m} \times 465.3 \mu\text{m}$ )



(b) EBSD orientation map acquired at a step size of  $0.5 \mu\text{m}$   
(Size of yellow rectangle =  $923.1 \mu\text{m} \times 465.3 \mu\text{m}$ )

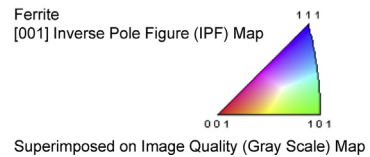
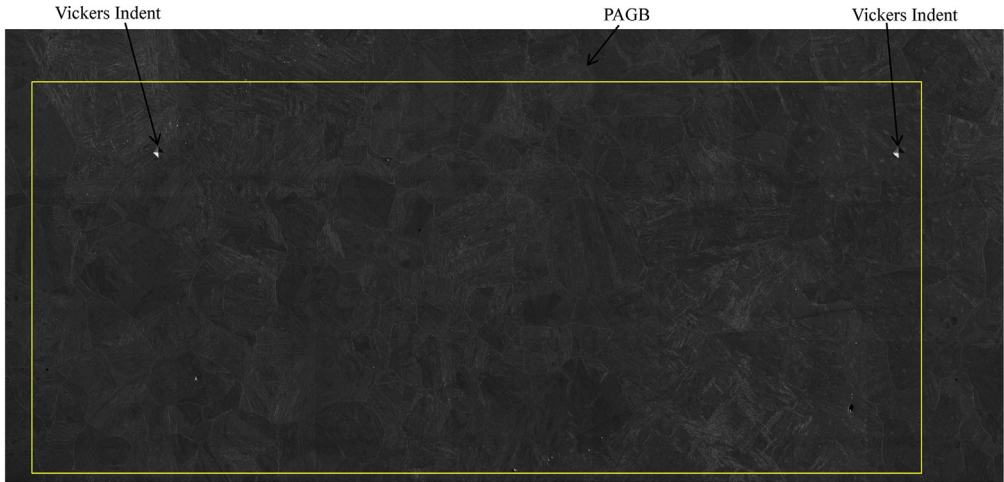
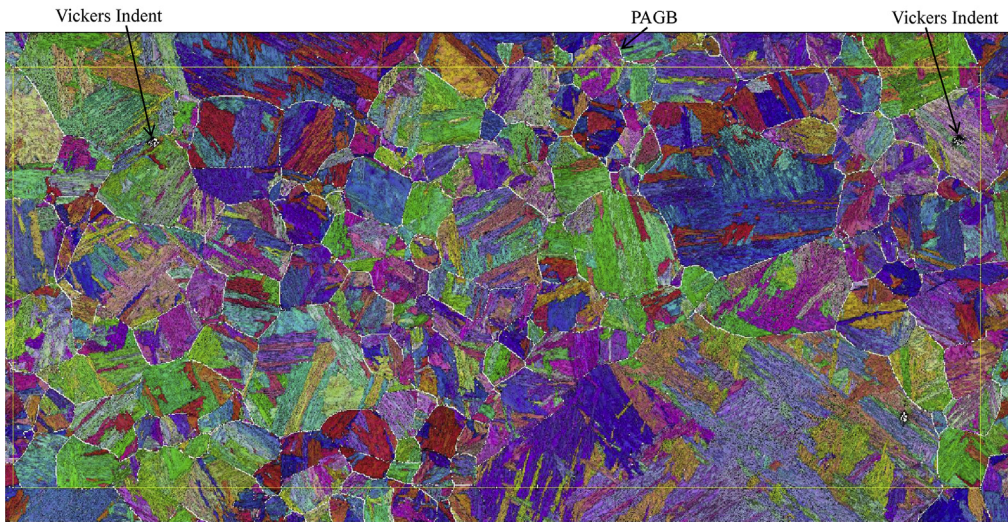


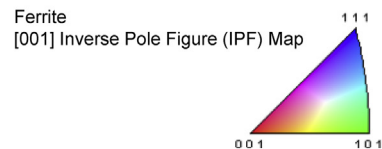
**Fig. 1.** Stitched (a) secondary electron SEM image and (b) EBSD orientation map of a large area on the specimen, which had been swab etched with a solution of 100 ml saturated aqueous picric acid and 0.5 g sodium dodecyl benzene sulfonate (a wetting agent) for 3 minutes. The area demarcated by yellow lines is cropped and analyzed as field of view 1 via stereological method. The prior austenite grain boundary (PAGB) triple points at two diagonally opposite corners (e.g., top-left and bottom-right) of the yellow rectangle aid consistency and minimize error, while cropping the same region of the specimen in the SEM image (a) and the corresponding EBSD map (b). The PAGBs are delineated in the EBSD map (b) as white lines for misorientations in the ranges  $19\text{--}48^\circ$  and  $61\text{--}62.8^\circ$ . The cropped SEM image and EBSD map with the gridlines for stereological analyses are presented in Ref. [1].



(a) SEM image (Size of yellow rectangle =  $968.2 \mu\text{m} \times 424.9 \mu\text{m}$ )



(b) EBSD orientation map acquired at a step size of  $0.5 \mu\text{m}$   
(Size of yellow rectangle =  $968.2 \mu\text{m} \times 424.9 \mu\text{m}$ )



Superimposed on Image Quality (Gray Scale) Map

**Fig. 2.** Stitched (a) secondary electron SEM image and (b) EBSD orientation map of a large area on the etched specimen. The area demarcated by yellow lines is cropped and analyzed as field of view 2 via stereological method. The grain boundary triple points at two diagonally opposite corners (e.g., top-left and bottom-right) of the yellow rectangle aid consistency and minimize error, while cropping the same region of the specimen in the SEM image (a) and the corresponding EBSD map (b). The PAGBs are delineated in the EBSD map (b) as white lines for misorientations in the ranges  $19\text{--}48^\circ$  and  $61\text{--}62.8^\circ$ . The cropped SEM image and EBSD map with the gridlines for stereological analyses are presented in Fig. 3.

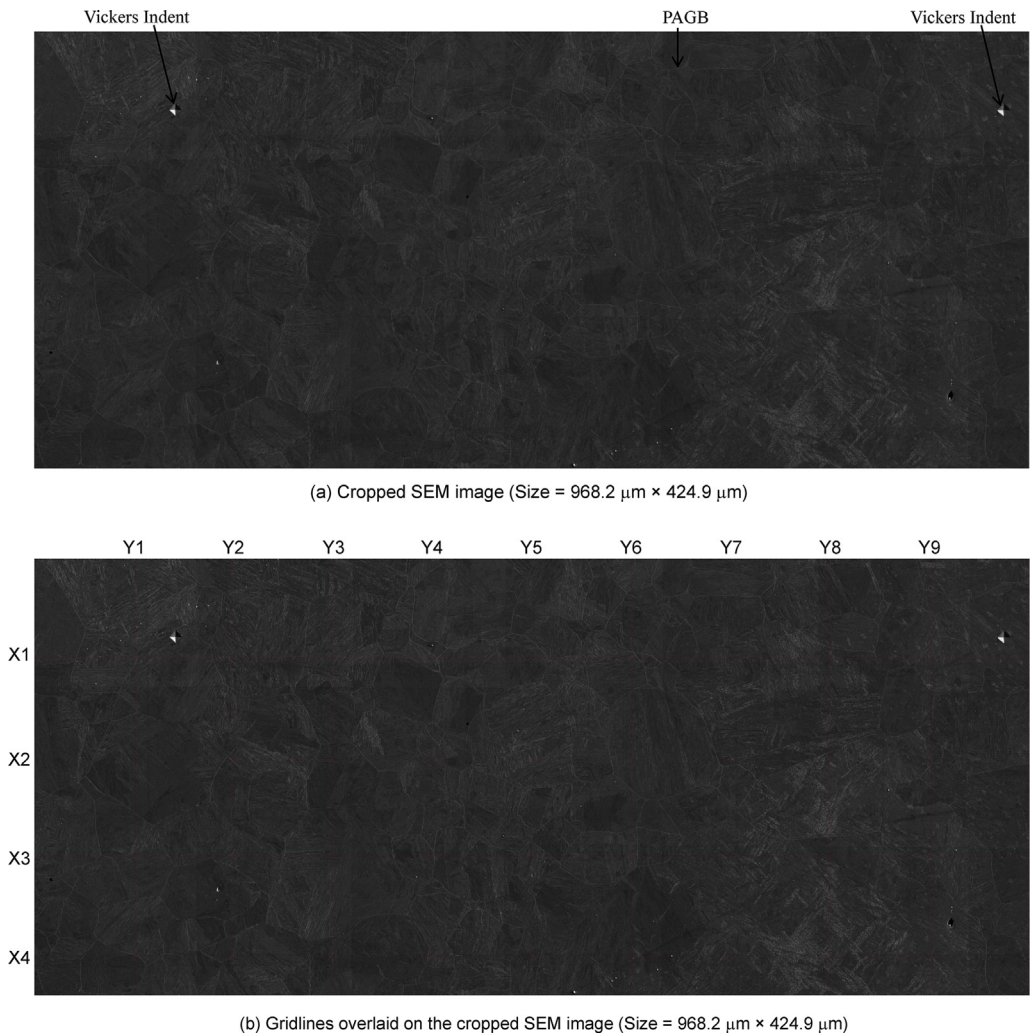


**Fig. 3.** Correlative microscopy for field of view 2. (a) Cropped SEM image of the region outlined by yellow rectangle in Fig. 2, (b) horizontal and vertical gridlines overlaid on the cropped SEM image to facilitate stereological analyses, (c) cropped EBSD orientation map of the region outlined by yellow rectangle in Fig. 2, and (d) horizontal and vertical gridlines overlaid on the cropped EBSD map to facilitate stereological analyses. The PAGBs are delineated in the EBSD maps ((c) and (d)) as white lines for misorientations in the ranges 19–48° and 61–62.8°.

The field of view 2 is outlined by a yellow rectangle in the large area SEM image (Fig. 2(a)) and the corresponding EBSD orientation map (Fig. 2(b)). The SEM image and EBSD map for the cropped region (i.e., field of view 2) are presented in Fig. 3. The horizontal and vertical gridlines overlaid on the cropped SEM image and EBSD map are also shown in Fig. 3. The results of stereological analyses on SEM image and EBSD map for field of view '2' are presented in Table 1.

Similarly, the fields of view 3, 4, and 5 are outlined by a yellow rectangle in Figs. 4, 6, and 8, respectively. The cropped SEM image and EBSD map for the fields of view 3, 4, and 5 are presented in Figs. 5, 7, and 9, respectively. The horizontal and vertical gridlines overlaid for stereological analyses on the fields of view 3, 4, and 5 are also shown in Figs. 5, 7, and 9, respectively. The results of stereological

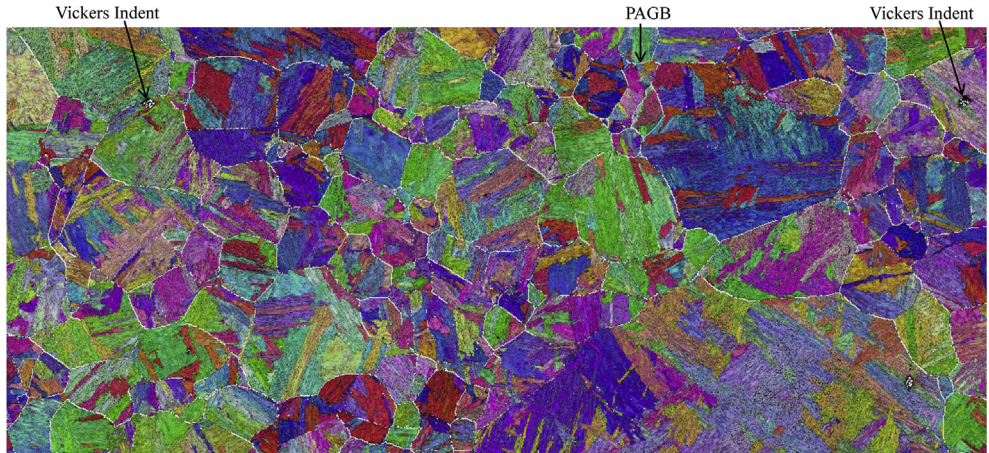
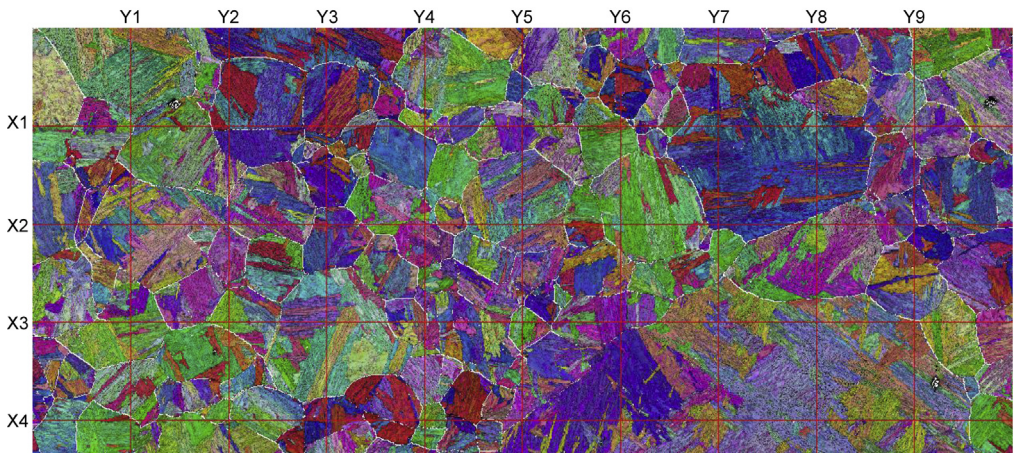
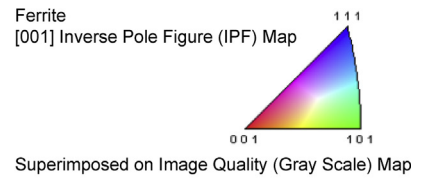
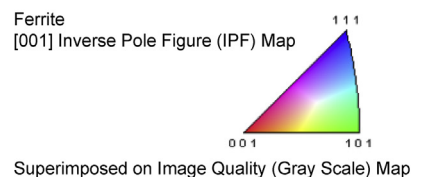
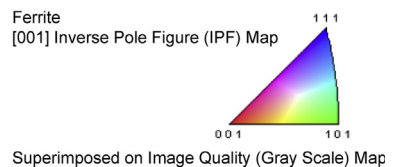
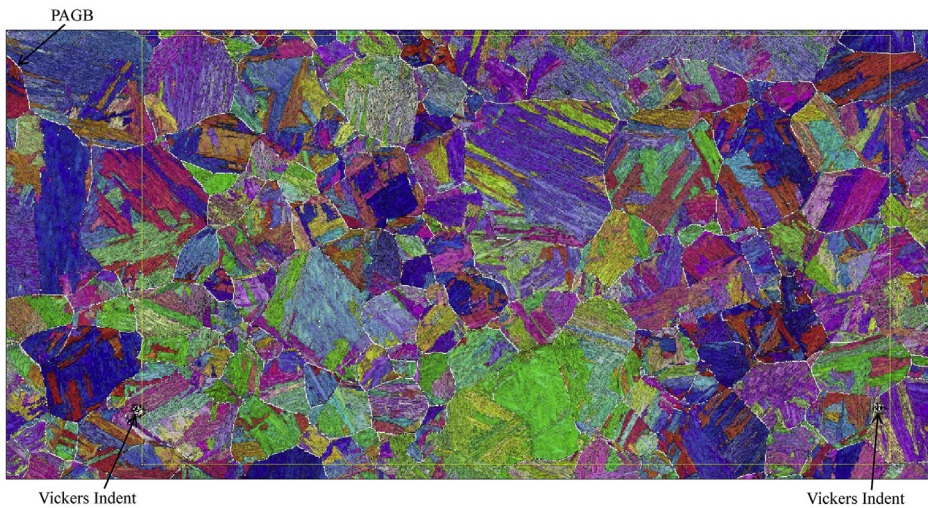
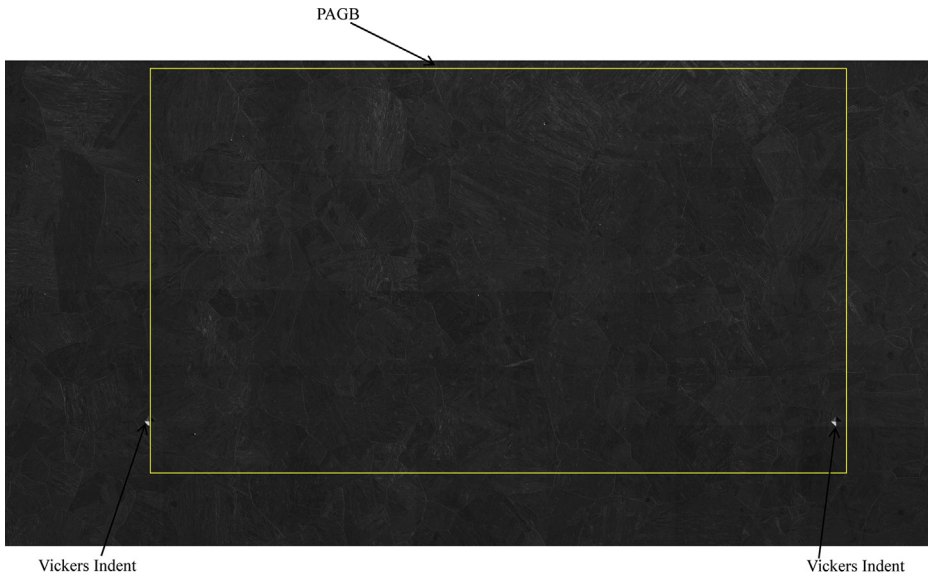
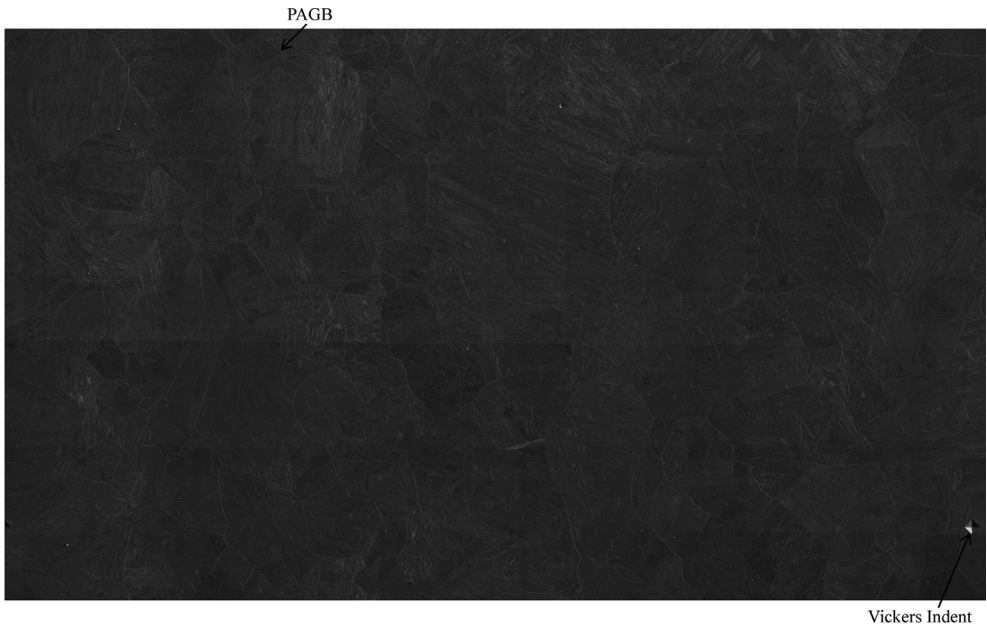
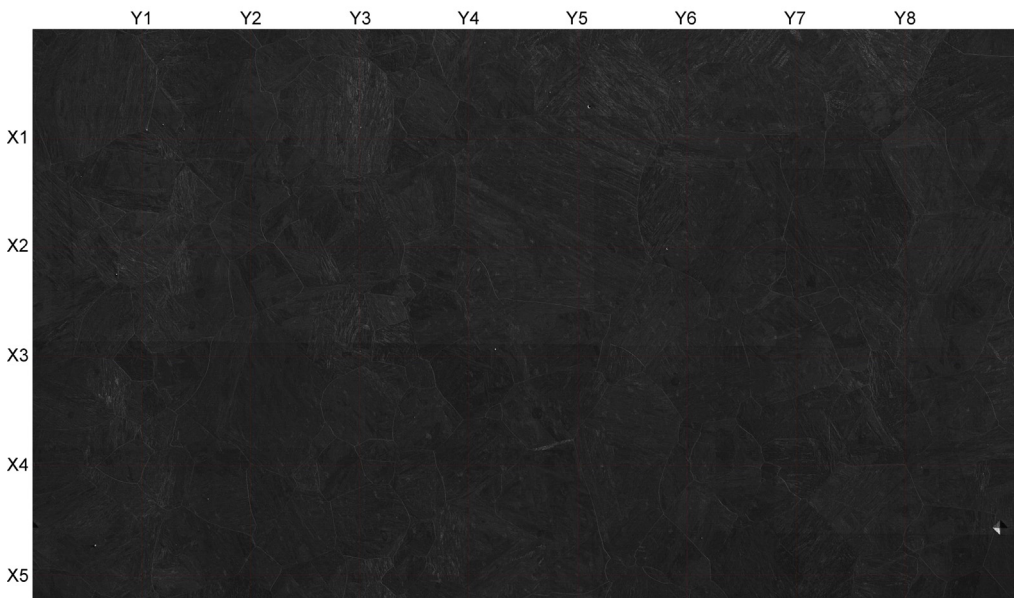
(c) Cropped EBSD orientation map (Size = 968.2  $\mu\text{m}$   $\times$  424.9  $\mu\text{m}$ )(d) Gridlines overlaid on the cropped EBSD orientation map (Size = 968.2  $\mu\text{m}$   $\times$  424.9  $\mu\text{m}$ )

Fig. 3. (continued).



**Fig. 4.** Stitched (a) secondary electron SEM image and (b) EBSD orientation map of a large area on the etched specimen. The area demarcated by yellow lines is cropped and analyzed as field of view 3 via stereological method. The grain boundary triple points at two diagonally opposite corners (e.g., top-left and bottom-right) of the yellow rectangle aid consistency and minimize error, while cropping the same region of the specimen in the SEM image (a) and the corresponding EBSD map (b). The PAGBs are delineated in the EBSD map (b) as white lines for misorientations in the ranges 19–48° and 61–62.8°. The cropped SEM image and EBSD map with the gridlines for stereological analyses are presented in Fig. 5.

(a) Cropped SEM image (Size = 817.6  $\mu\text{m}$   $\times$  476.0  $\mu\text{m}$ )(b) Gridlines overlaid on the cropped SEM image (Size = 817.6  $\mu\text{m}$   $\times$  476.0  $\mu\text{m}$ )

**Fig. 5.** Correlative microscopy for field of view 3. (a) Cropped SEM image of the region outlined by yellow rectangle in Fig. 4, (b) horizontal and vertical gridlines overlaid on the cropped SEM image to facilitate stereological analyses, (c) cropped EBSD orientation map of the region outlined by yellow rectangle in Fig. 4, and (d) horizontal and vertical gridlines overlaid on the cropped EBSD map to facilitate stereological analyses. The PAGBs are delineated in the EBSD maps ((c) and (d)) as white lines for misorientations in the ranges 19–48° and 61–62.8°.

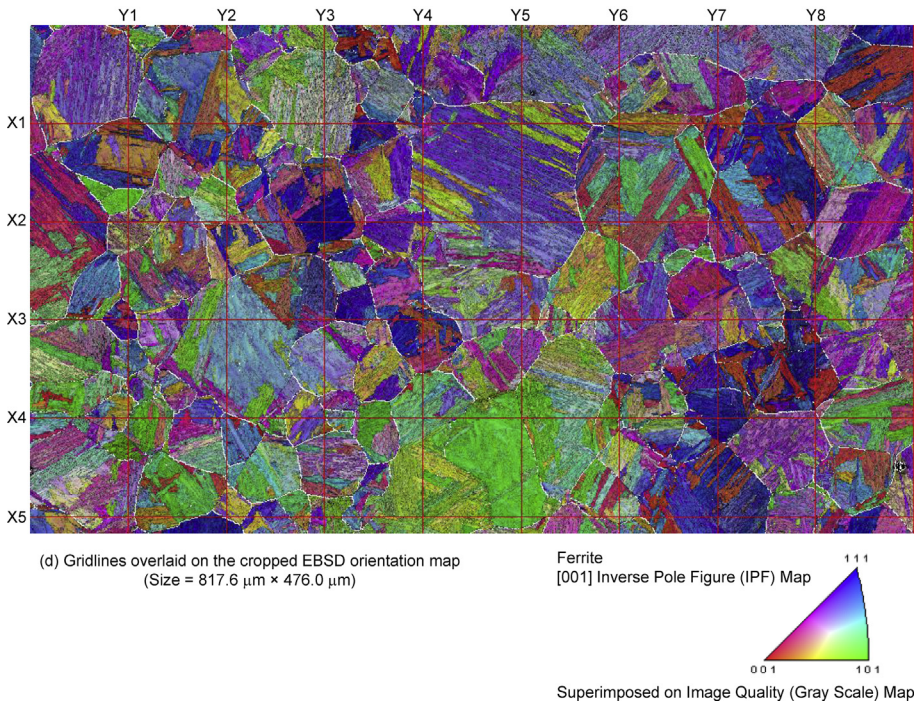
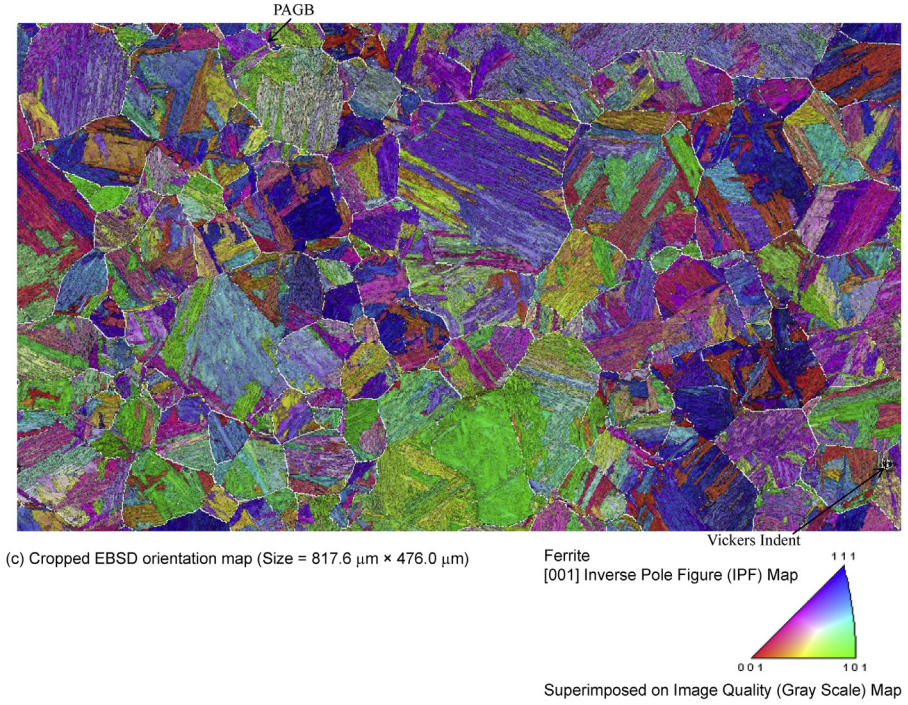
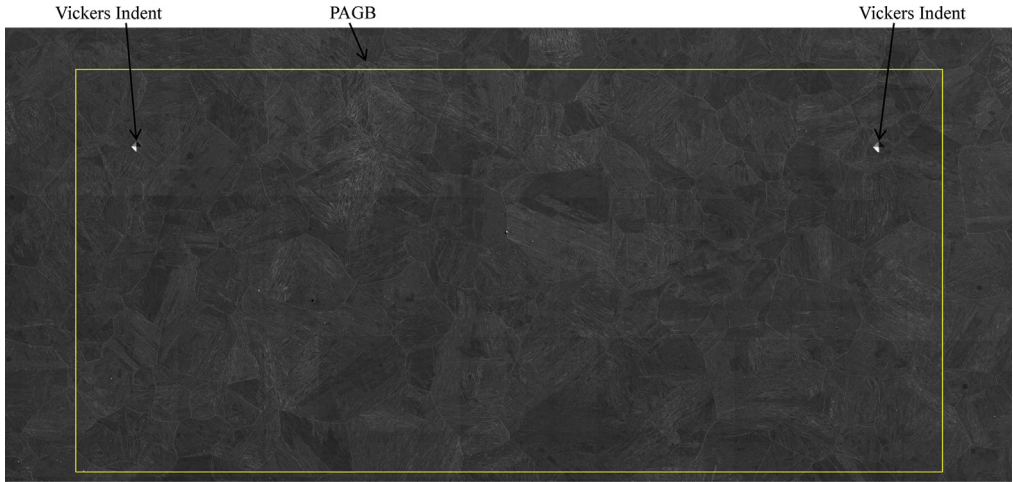
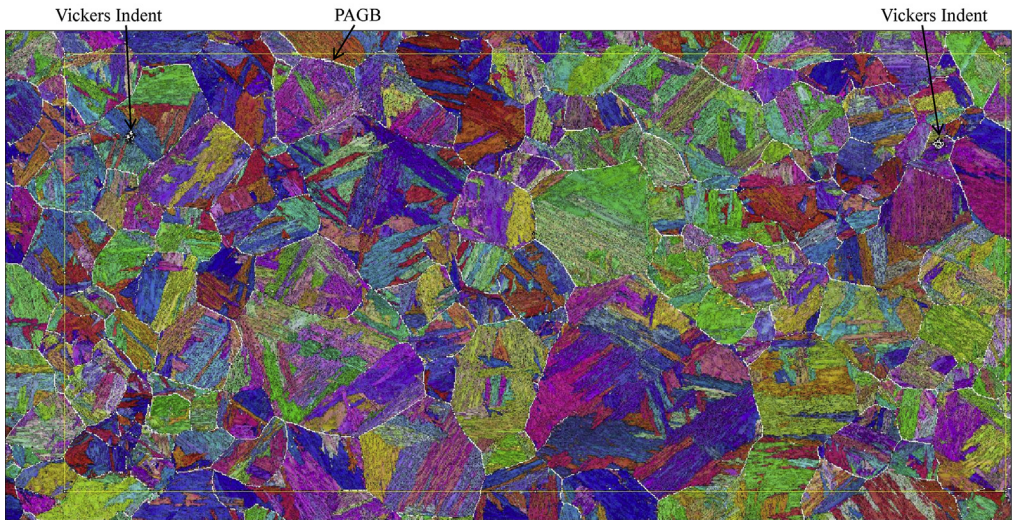


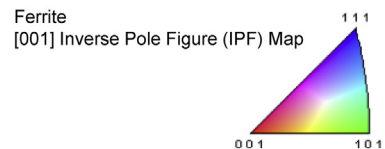
Fig. 5. (continued).



(a) SEM image (Size of yellow rectangle =  $939.4 \mu\text{m} \times 436.0 \mu\text{m}$ )



(b) EBSD orientation map acquired at a step size of  $0.5 \mu\text{m}$   
(Size of yellow rectangle =  $939.4 \mu\text{m} \times 436.0 \mu\text{m}$ )



Superimposed on Image Quality (Gray Scale) Map

**Fig. 6.** Stitched (a) secondary electron SEM image and (b) EBSD orientation map of a large area on the etched specimen. The area demarcated by yellow lines is cropped and analyzed as field of view 4 via stereological method. The grain boundary triple points at two diagonally opposite corners (e.g., top-left and bottom-right) of the yellow rectangle aid consistency and minimize error, while cropping the same region of the specimen in the SEM image (a) and the corresponding EBSD map (b). The PAGBs are delineated in the EBSD map (b) as white lines for misorientations in the ranges  $19\text{--}48^\circ$  and  $61\text{--}62.8^\circ$ . The cropped SEM image and EBSD map with the gridlines for stereological analyses are presented in Fig. 7.

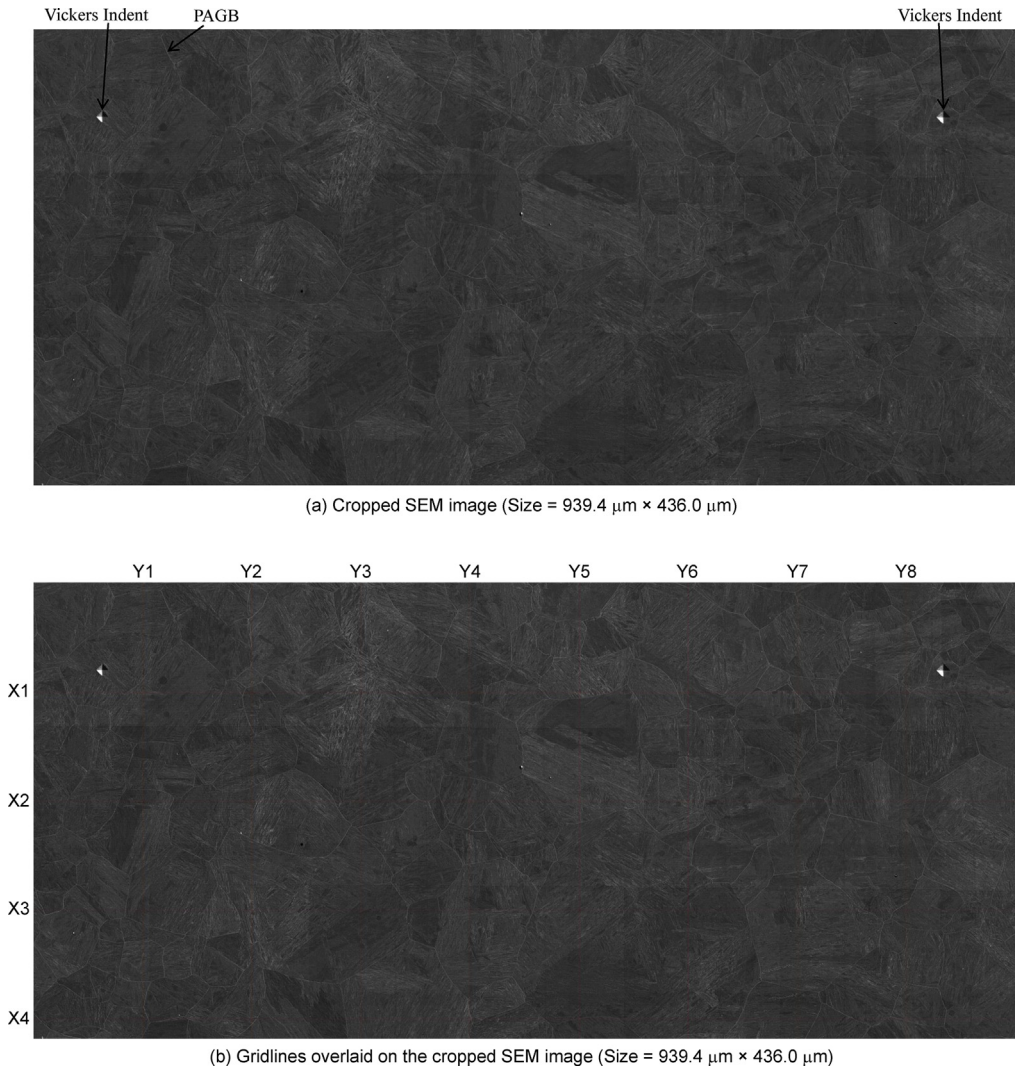


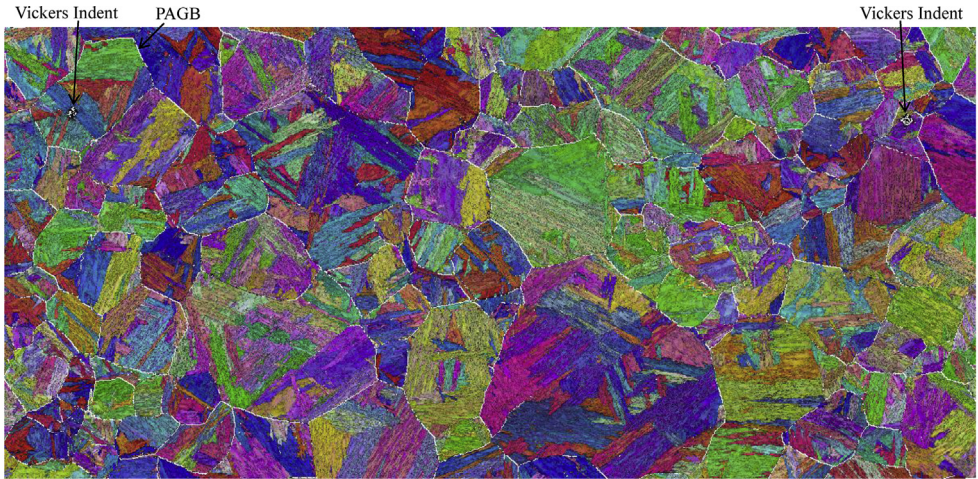
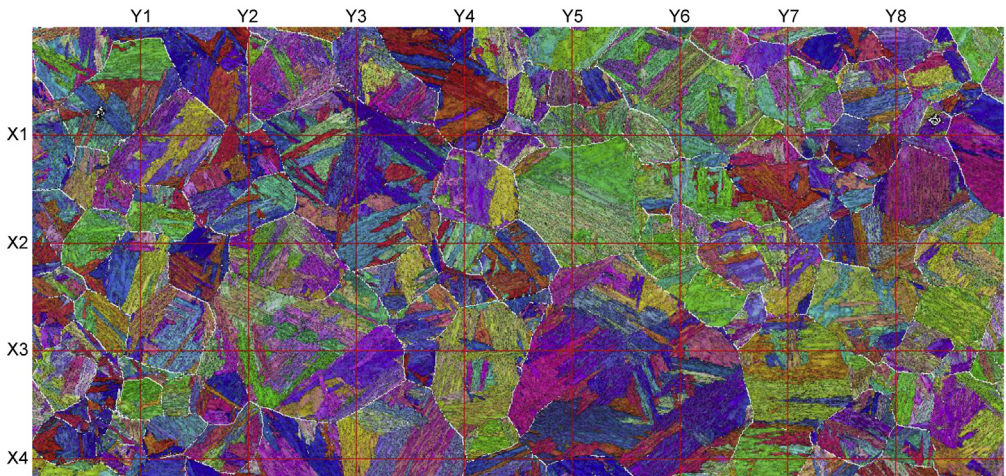
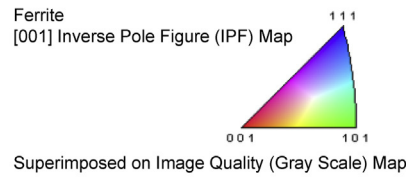
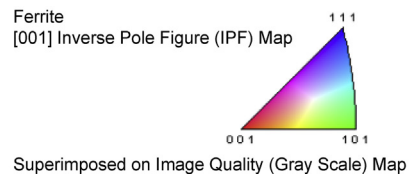
**Fig. 7.** Correlative microscopy for field of view 4. (a) Cropped SEM image of the region outlined by yellow rectangle in Fig. 6, (b) horizontal and vertical gridlines overlaid on the cropped SEM image to facilitate stereological analyses, (c) cropped EBSD orientation map of the region outlined by yellow rectangle in Fig. 6, and (d) horizontal and vertical gridlines overlaid on the cropped EBSD map to facilitate stereological analyses. The PAGBs are delineated in the EBSD maps ((c) and (d)) as white lines for misorientations in the ranges 19–48° and 61–62.8°.

analyses on SEM images and EBSD maps for fields of view 3, 4, and 5 are presented in Tables 2, 3, and 4, respectively.

The links for downloading high resolution SEM images and EBSD scan data (both raw and cleaned) for the five fields of view are provided in Table 5.

## 2. Experimental design, materials, and methods

The material for this study was a low-alloy high-performance martensitic steel (AF 9628). The chemical composition and heat treatment steps are reported elsewhere [1,5]. To reveal the PAGBs in the

(c) Cropped EBSD orientation map (Size = 939.4  $\mu\text{m}$   $\times$  436.0  $\mu\text{m}$ )(d) Gridlines overlaid on the cropped EBSD orientation map (Size = 939.4  $\mu\text{m}$   $\times$  436.0  $\mu\text{m}$ )**Fig. 7.** (continued).

**Table 1**

Stereological analyses on SEM image and EBSD map for field of view '2' (i.e., Fig. 3).

Test line ID	Line length ( $\mu\text{m}$ )	Etching and SEM Imaging			Misorientation Thresholding in EBSD Maps		
		Number of intersections	Mean lineal intercept length ( $\mu\text{m}$ )	$P_L$ = Number of intersections generated per unit length of test lines ( $\text{mm}^{-1}$ )	Number of intersections	Mean lineal intercept length ( $\mu\text{m}$ )	$P_L$ = Number of intersections generated per unit length of test lines ( $\text{mm}^{-1}$ )
X1	968.2	21.5	45.0	22.2	20	48.4	20.7
X2	968.2	18	53.8	18.6	17.5	55.3	18.1
X3	968.2	14.5	66.8	15.0	12.5	77.5	12.9
X4	968.2	14	69.2	14.5	16.5	58.7	17.0
Y1	424.9	8	53.1	18.8	5	85.0	11.8
Y2	424.9	9.5	44.7	22.4	9.5	44.7	22.4
Y3	424.9	6.5	65.4	15.3	5.5	77.3	12.9
Y4	424.9	15	28.3	35.3	8	53.1	18.8
Y5	424.9	11.5	37.0	27.1	10	42.5	23.5
Y6	424.9	6	70.8	14.1	6.5	65.4	15.3
Y7	424.9	5	85.0	11.8	3	141.6	7.1
Y8	424.9	5	85.0	11.8	4	106.2	9.4
Y9	424.9	11	38.6	25.9	7	60.7	16.5
<b>For the entire field of view</b>	<b>7697.1</b>	<b>145.5</b>	<b>52.9</b>	<b>18.9</b>	<b>125</b>	<b>61.6</b>	<b>16.2</b>

Note: X1 is the topmost horizontal line and Y1 is the leftmost vertical line.

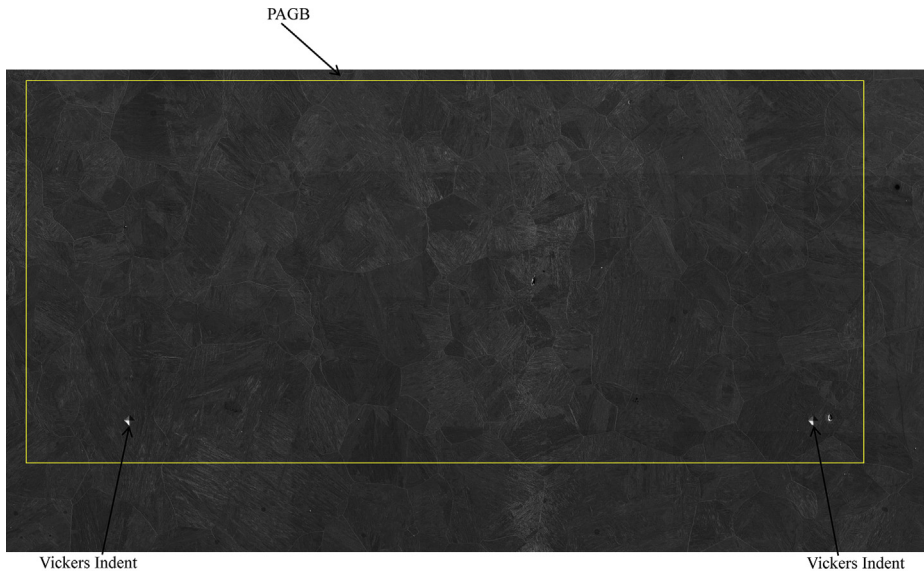
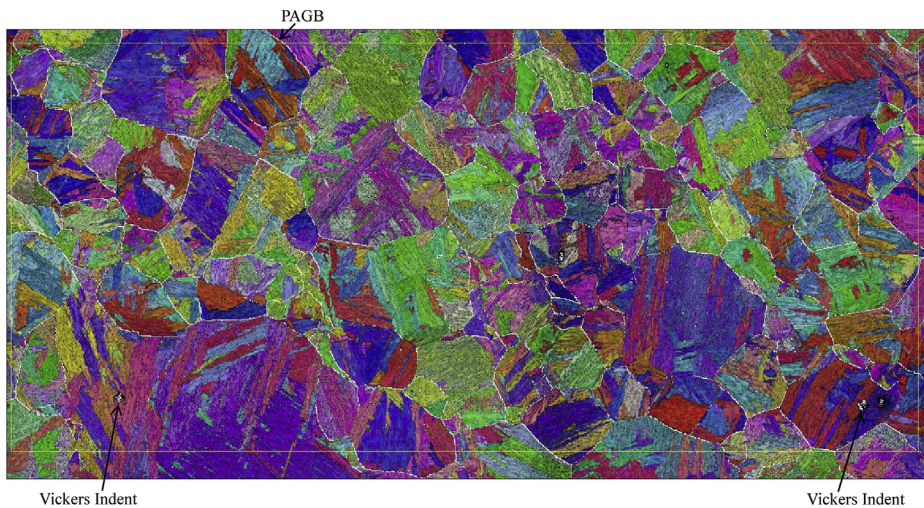
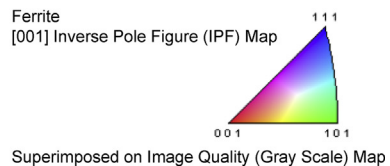
**Table 2**

Stereological analyses on SEM image and EBSD map for field of view '3' (i.e., Fig. 5).

Test line ID	Line length ( $\mu\text{m}$ )	Etching and SEM Imaging			Misorientation Thresholding in EBSD Maps		
		Number of intersections	Mean lineal intercept length ( $\mu\text{m}$ )	$P_L$ = Number of intersections generated per unit length of test lines ( $\text{mm}^{-1}$ )	Number of intersections	Mean lineal intercept length ( $\mu\text{m}$ )	$P_L$ = Number of intersections generated per unit length of test lines ( $\text{mm}^{-1}$ )
X1	817.6	15.5	52.7	19.0	12	68.1	14.7
X2	817.6	13	62.9	15.9	10	81.8	12.2
X3	817.6	17.5	46.7	21.4	17.5	46.7	21.4
X4	817.6	21	38.9	25.7	14.5	56.4	17.7
X5	817.6	19	43.0	23.2	16.5	49.5	20.2
Y1	476.0	13	36.6	27.3	10.5	45.3	22.1
Y2	476.0	11	43.3	23.1	9	52.9	18.9
Y3	476.0	9.5	50.1	20.0	7.5	63.5	15.8
Y4	476.0	10	47.6	21.0	5	95.2	10.5
Y5	476.0	6	79.3	12.6	6	79.3	12.6
Y6	476.0	8	59.5	16.8	9	52.9	18.9
Y7	476.0	9	52.9	18.9	9	52.9	18.9
Y8	476.0	12.5	38.1	26.3	10.5	45.3	22.1
<b>For the entire field of view</b>	<b>7896.1</b>	<b>165</b>	<b>47.9</b>	<b>20.9</b>	<b>137</b>	<b>57.6</b>	<b>17.4</b>

Note: X1 is the topmost horizontal line and Y1 is the leftmost vertical line.

SEM images, the heat treated specimen was swab etched with a solution of 100 ml saturated aqueous picric acid and 0.5 g sodium dodecyl benzene sulfonate (a wetting agent) for 3 minutes, as described earlier [1,5]. The correlative microscopy methodology to acquire large area SEM images and

(a) SEM image (Size of yellow rectangle = 989.9  $\mu\text{m}$   $\times$  451.0  $\mu\text{m}$ )(b) EBSD orientation map acquired at a step size of 0.5  $\mu\text{m}$   
(Size of yellow rectangle = 989.9  $\mu\text{m}$   $\times$  451.0  $\mu\text{m}$ )

**Fig. 8.** Stitched (a) secondary electron SEM image and (b) EBSD orientation map of a large area on the etched specimen. The area demarcated by yellow lines is cropped and analyzed as field of view 5 via stereological method. The grain boundary triple points at two diagonally opposite corners (e.g., top-left and bottom-right) of the yellow rectangle aid consistency and minimize error, while cropping the same region of the specimen in the SEM image (a) and the corresponding EBSD map (b). The PAGBs are delineated in the EBSD map (b) as white lines for misorientations in the ranges 19–48° and 61–62.8°. The cropped SEM image and EBSD map with the gridlines for stereological analyses are presented in Fig. 9.

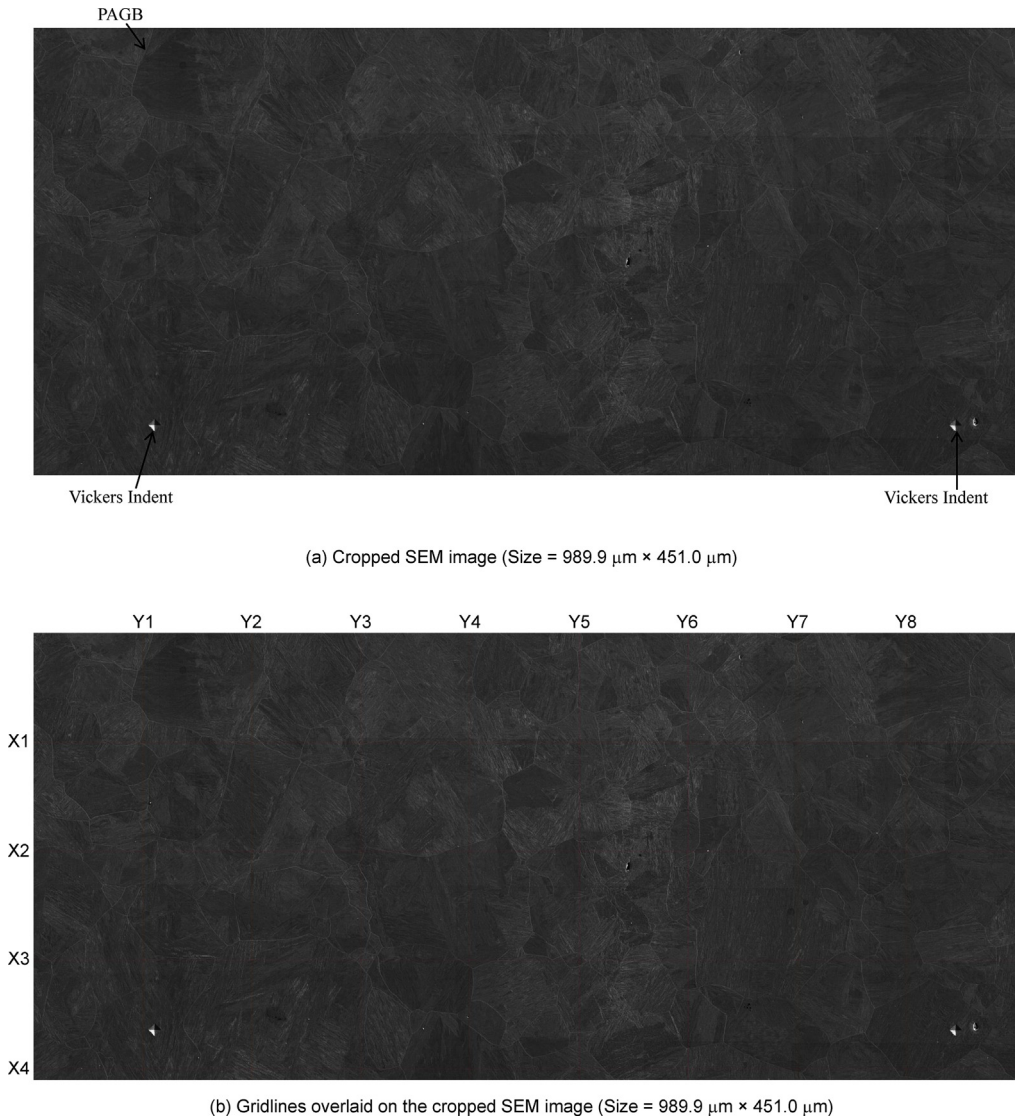
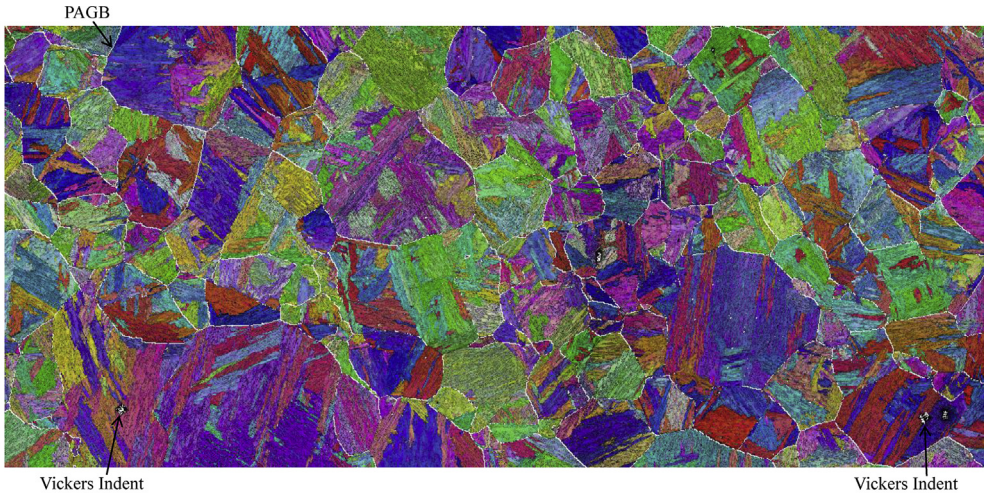


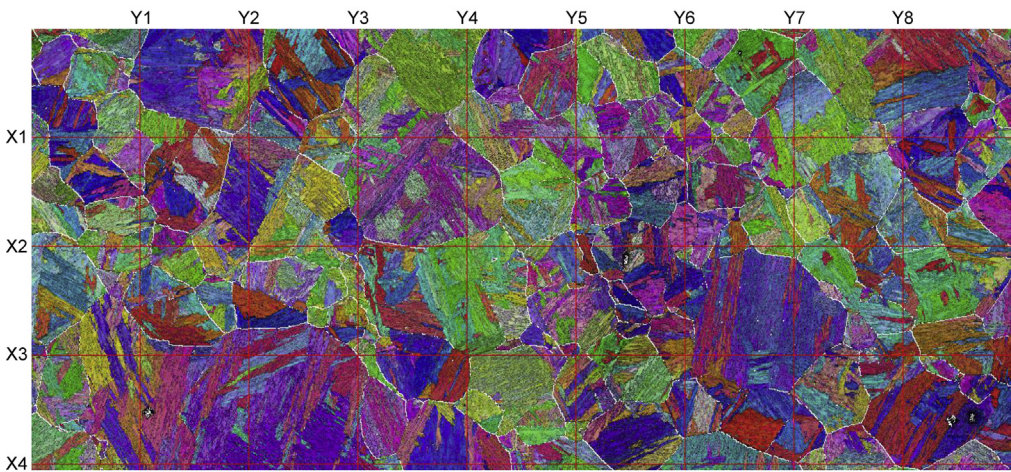
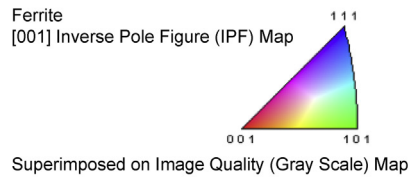
**Fig. 9.** Correlative microscopy for field of view 5. (a) Cropped SEM image of the region outlined by yellow rectangle in Fig. 8, (b) horizontal and vertical gridlines overlaid on the cropped SEM image to facilitate stereological analyses, (c) cropped EBSD orientation map of the region outlined by yellow rectangle in Fig. 8, and (d) horizontal and vertical gridlines overlaid on the cropped EBSD map to facilitate stereological analyses. The PAGBs are delineated in the EBSD maps ((c) and (d)) as white lines for misorientations in the ranges 19–48° and 61–62.8°.

corresponding EBSD orientation maps of the same areas of the specimen is described in detail in Section 2.2 of the accompanying research article [1] and is not repeated here.

It is extremely important to crop essentially the same area in the SEM image and the corresponding EBSD map to properly compare the stereological measurements on the two images. A zero-dimensional microstructural feature at each of the two diagonally opposite corners (i.e., either top-left and bottom-right or top-right and bottom-left) of a rectangle can serve as an ideal point to aid



(c) Cropped EBSD orientation map (Size = 989.9  $\mu\text{m}$   $\times$  451.0  $\mu\text{m}$ )



(d) Gridlines overlaid on the cropped EBSD orientation map  
(Size = 989.9  $\mu\text{m}$   $\times$  451.0  $\mu\text{m}$ )

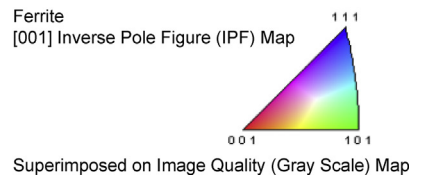


Fig. 9. (continued).

**Table 3**

Stereological analyses on SEM image and EBSD map for field of view '4' (i.e., Fig. 7).

Test line ID	Line length ( $\mu\text{m}$ )	Etching and SEM Imaging			Misorientation Thresholding in EBSD Maps		
		Number of intersections	Mean lineal intercept length ( $\mu\text{m}$ )	$P_L$ = Number of intersections generated per unit length of test lines ( $\text{mm}^{-1}$ )	Number of intersections	Mean lineal intercept length ( $\mu\text{m}$ )	$P_L$ = Number of intersections generated per unit length of test lines ( $\text{mm}^{-1}$ )
X1	939.4	18.5	50.8	19.7	16.5	56.9	17.6
X2	939.4	17.5	53.7	18.6	17	55.3	18.1
X3	939.4	16	58.7	17.0	12.5	75.2	13.3
X4	939.4	19.5	48.2	20.8	16	58.7	17.0
Y1	436.0	10.5	41.5	24.1	7	62.3	16.1
Y2	436.0	11.5	37.9	26.4	9	48.4	20.6
Y3	436.0	4	109.0	9.2	4	109.0	9.2
Y4	436.0	9	48.4	20.6	6	72.7	13.8
Y5	436.0	5	87.2	11.5	5	87.2	11.5
Y6	436.0	9	48.4	20.6	6.5	67.1	14.9
Y7	436.0	10	43.6	22.9	8	54.5	18.3
Y8	436.0	11.5	37.9	26.4	6.5	67.1	14.9
<b>For the entire field of view</b>	<b>7245.9</b>	<b>142</b>	<b>51.0</b>	<b>19.6</b>	<b>114</b>	<b>63.6</b>	<b>15.7</b>

Note: X1 is the topmost horizontal line and Y1 is the leftmost vertical line.

**Table 4**

Stereological analyses on SEM image and EBSD map for field of view '5' (i.e., Fig. 9).

Test line ID	Line length ( $\mu\text{m}$ )	Etching and SEM Imaging			Misorientation Thresholding in EBSD Maps		
		Number of intersections	Mean lineal intercept length ( $\mu\text{m}$ )	$P_L$ = Number of intersections generated per unit length of test lines ( $\text{mm}^{-1}$ )	Number of intersections	Mean lineal intercept length ( $\mu\text{m}$ )	$P_L$ = Number of intersections generated per unit length of test lines ( $\text{mm}^{-1}$ )
X1	989.9	24	41.2	24.2	16	61.9	16.2
X2	989.9	23.5	42.1	23.7	21.5	46.0	21.7
X3	989.9	18.5	53.5	18.7	12	82.5	12.1
X4	989.9	15	66.0	15.2	9	110.0	9.1
Y1	451.0	10	45.1	22.2	9	50.1	20.0
Y2	451.0	4	112.8	8.9	5	90.2	11.1
Y3	451.0	10	45.1	22.2	9	50.1	20.0
Y4	451.0	6	75.2	13.3	4	112.8	8.9
Y5	451.0	11.5	39.2	25.5	10.5	43.0	23.3
Y6	451.0	11	41.0	24.4	8	56.4	17.7
Y7	451.0	9.5	47.5	21.1	9	50.1	20.0
Y8	451.0	9	50.1	20.0	7.5	60.1	16.6
<b>For the entire field of view</b>	<b>7568.1</b>	<b>152</b>	<b>49.8</b>	<b>20.1</b>	<b>120.5</b>	<b>62.8</b>	<b>15.9</b>

Note: X1 is the topmost horizontal line and Y1 is the leftmost vertical line.

cropping of the same region on the specimen surface in the SEM image and the corresponding EBSD map. In this study, the PAGB triple points were selected as zero-dimensional microstructural features to aid cropping of the same region in the SEM image and the corresponding EBSD map. This is depicted by a yellow rectangle in Figs. 1, 2, 4, 6, and 8 for fields of view 1, 2, 3, 4, and 5, respectively.

**Table 5**

Links for downloading high resolution SEM images and EBSD scan data.

Field of view	Size of field of view		Figure for Stereological Analyses	Table for Stereological Analyses	Links for downloading high resolution SEM images <sup>a</sup>	Links for downloading raw and cleaned <sup>b</sup> EBSD scan data <sup>c,d,e</sup>
	Width (μm)	Height (μm)				
1	923.1	465.3	Fig. 7 of Ref. [1]	Table 2 in Ref. [1]	Links for 'Field of view 1_High Res SEM image.tif' and 'Field of view 1_High Res SEM image_with grid overlay.tif' are in Ref. [8]	Links for 'Field of view 1_EBSD data_Raw.ang' and 'Field of view 1_EBSD data_Cleaned.ang' are in Ref. [8]
2	968.2	424.9	Fig. 3	Table 1	Links for 'Field of view 2_High Res SEM image.tif' and 'Field of view 2_High Res SEM image_with grid overlay.tif' are in Ref. [8]	Links for 'Field of view 2_EBSD data_Raw.ang' and 'Field of view 2_EBSD data_Cleaned.ang' are in Ref. [8]
3	817.6	476.0	Fig. 5	Table 2	Links for 'Field of view 3_High Res SEM image.tif' and 'Field of view 3_High Res SEM image_with grid overlay.tif' are in Ref. [8]	Links for 'Field of view 3_EBSD data_Raw.ang' and 'Field of view 3_EBSD data_Cleaned.ang' are in Ref. [8]
4	939.4	436.0	Fig. 7	Table 3	Links for 'Field of view 4_High Res SEM image.tif' and 'Field of view 4_High Res SEM image_with grid overlay.tif' are in Ref. [8]	Links for 'Field of view 4_EBSD data_Raw.ang' and 'Field of view 4_EBSD data_Cleaned.ang' are in Ref. [8]
5	989.9	451.0	Fig. 9	Table 4	Links for 'Field of view 5_High Res SEM image.tif' and 'Field of view 5_High Res SEM image_with grid overlay.tif' are in Ref. [8]	Links for 'Field of view 5_EBSD data_Raw.ang' and 'Field of view 5_EBSD data_Cleaned.ang' are in Ref. [8]

<sup>a</sup> The high resolution SEM images, provided for download, are for the cropped regions shown in Fig. 4 of Ref. [1], Figs. 3(a,b), 5(a,b), 7(a,b), and 9(a,b) for the fields of view 1, 2, 3, 4, and 5, respectively.

<sup>b</sup> The raw EBSD scan data were cleaned using "neighbor CI correlation" cleanup method with a minimum confidence index (CI) of 0.2 and are provided as the cleaned EBSD scan data.

<sup>c</sup> The EBSD scan area is slightly larger than the respective fields of view. The EBSD scan areas, for which the crystallographic orientation data (\*.ang files) are provided, are shown in Figs. 1(b), 2(b), 4(b), 6(b), and 8(b) for fields of view 1, 2, 3, 4, and 5, respectively. The EBSD scan areas need to be cropped, as shown by yellow rectangle in Figs. 1(b), 2(b), 4(b), 6(b), and 8(b), to obtain the fields of view corresponding to the high resolution SEM images provided for download. Only after cropping, the EBSD scan areas will have the correct width and height for their respective fields of view, and the cropped EBSD maps will match the areas of the high resolution SEM images provided for download.

<sup>d</sup> It should be emphasized that the micron bar from the EBSD data file (\*.ang file) should not be used for stereological analyses because it may lead to error in measurements. As explained in Section 2.3 of Ref. [1], the sizes (widths and heights) of cropped regions for the five fields of view were calculated from the calibrated SEM images and are accurate within  $\pm 2\%$ . Thereafter, the same line lengths of individual gridlines were used for stereological measurements on cropped SEM images and corresponding EBSD maps (Table 2 of Ref. [1], Tables 1–4) to obtain consistent results with minimal error.

<sup>e</sup> The EBSD data files (\*.ang) have data in 10 columns. The columns 1, 2, and 3 are Euler angles  $\phi_1$ ,  $\phi$ , and  $\phi_2$ , respectively, in radians in Bunge's notation. Columns 4 and 5 are the horizontal (x) and the vertical (y) coordinates, respectively, of the points in scan, in micrometers. Columns 6 and 7 are the image quality and confidence index, respectively. Columns 8, 9, and 10 are phase identifier, detector intensity, and fit, respectively.

The gridlines were overlaid on the cropped SEM images and EBSD maps using ImageJ [6]. The gridlines were equidistant in both the horizontal and vertical directions in a given image, and their locations were consistent in an SEM image and the corresponding EBSD map (Fig. 7 of Ref. [1], Figs. 3, 5, 7, and 9).

The intersections between gridlines and PAGBs were counted per the recommendations of ASTM E112 – 13 [7]. Specifically, a tangential intersection of the test line with a PAGB was counted as 1 intersection. An intersection of the gridline with a PAGB triple point was counted as 1.5 intersections. When the end of a test line touched a PAGB, it was counted as 0.5 intersection. If the ends of a gridline did not touch a PAGB, they were not counted as intersections. The number of intersections between the individual test lines and PAGBs are presented in Table 2 of Ref. [1], Tables 1, 2, 3, and 4 for fields of view 1, 2, 3, 4, and 5, respectively.

## Acknowledgments

This research was supported by and performed at the Air Force Research Laboratory, Materials and Manufacturing Directorate, AFRL/RXCM, Wright-Patterson Air Force Base, OH, USA. The authors thank Mr. Tommy Cissel (formerly with UES, Inc.) and Mr. Bob Lewis (formerly with UES, Inc.) for help with specimen preparations, and Mr. Jared Shank (UES, Inc.) for help with EBSD experiments. The authors thank Dr. R.A. Abrahams (AFLCMC) for providing AF9628 steel examined in this study. The authors also thank Mr. George F. Vander Voort and Prof. George Krauss (Colorado School of Mines) for helpful suggestions on etching techniques.

## Conflict of Interest

The authors declare that they have no known competing financial interests or personal relationships that could have appeared to influence the work reported in this paper.

## References

- [1] V. Sinha, M. Gonzales, R.A. Abrahams, B.S. Song, E.J. Payton, Correlative microscopy for quantification of prior austenite grain size in AF9628 steel, *Mater. Char.* (2019), <https://doi.org/10.1016/j.matchar.2019.109835> (In Press).
- [2] Cyril Cayron, ARPGE: a computer program to automatically reconstruct the parent grains from electron backscatter diffraction data, *J. Appl. Crystallogr.* 40 (2007) 1183–1188.
- [3] Goro Miyamoto, Naomichi Iwata, Naoki Takayama, Tadashi Furuhashi, Mapping the parent austenite orientation reconstructed from the orientation of martensite by EBSD and its application to ausformed martensite, *Acta Mater.* 58 (2010) 6393–6403.
- [4] L. Germain, N. Gey, R. Mercier, P. Blaineau, M. Humbert, An advanced approach to reconstructing parent orientation maps in the case of approximate orientation relations: application to steels, *Acta Mater.* 60 (2012) 4551–4562.
- [5] V. Sinha, E.J. Payton, M. Gonzales, R.A. Abrahams, B.S. Song, Delineation of prior austenite grain boundaries in a low-alloy high-performance steel, *Metallogr. Microstruct. Anal.* 6 (6) (2017) 610–618. <https://doi.org/10.1007/s13632-017-0403-4>.
- [6] <https://imagej.nih.gov/ij/>. (Accessed 10 May 2019).
- [7] ASTM E112 – 13, Standard Test Methods for Determining Average, Grain Size, Developed by Subcommittee E04.08 on Grain Size, ASTM International, West Conshohocken, PA, USA, 2013. <https://doi.org/10.1520/E0112-13>.
- [8] V. Sinha, M. Gonzales, E.J. Payton, Correlative microscopy data for quantification of prior austenite grain size in AF9628 steel, Dataset uploaded on materials data facility repository. <https://doi.org/10.18126/iv89-3293>, 2019.